The digital endocast of *Necrolemur antiquus*

Arianna R. Harrington[a¶], Gabriel S. Yapuncich[a¶*], Doug M. Boyer[a]

[a]Department of Evolutionary Anthropology, Box 90383, Duke University, Durham, NC 27708, USA

¶These authors contributed equally to this work

*corresponding author: gabrielyapuncich@gmail.com

Abstract: The study of endocasts, or casts of the endocranial space, have played an important role in shaping understanding of mammalian, and particularly primate, brain evolution. Recently, the reconstructions of three-dimensional virtual endocasts from high-resolution computed tomography images have allowed for the visualization and quantification of endocasts in several Paleocene and Eocene primate species. Here we present the virtual endocast of MaPhQ 289 (informally known as the Montauban 9 skull), a specimen of *Necrolemur antiquus* Filhol 1873, a middle to late Eocene European primate of the family Microchoeridae. The virtual endocast of MaPhQ 289 reveals a lissencephalic surface morphology with expanded temporal poles and minimal overlap of the cerebellum or olfactory bulb by the cerebrum, which closely resembles the morphology of the endocast of its contemporary relative, *Microchoerus erinaceus* (Primates, Microchoeridae). MaPhQ 289 yields an endocranial volume (ECV) of 2.36 cm^3, about 60% smaller than the volume of the most commonly cited ECV of *N. antiquus*. Thus, the size of the brain of *N. antiquus* relative to its body size is likely to be smaller than has been reported in previous literature, highlighting the importance of corroborating older ECV estimates with new evidence using 3-D imaging techniques. Finally, the digitally prepared endocast reveals that the promontorial canal for the internal carotid artery was relatively more enlarged than previously appreciated, suggesting that later-occurring microchoerids (such as *Microchoerus*) reduced their reliance on the promontory artery for cerebral blood.

Keywords: Primates, brain evolution, omomyiforms, Eocene

INTRODUCTION

Among mammals, primates are notable for their relatively large and reorganized brains (Martin, 1990; Barton, 2006). Understanding the "tempo and mode" (Simpson, 1944) of primate brain evolution has long been an area of intense research (Clutton-Brock & Harvey, 1980; Dunbar, 1998; Healy & Rowe, 2007). Despite sustained interest in the evolutionary history of the primate brain, there are only a handful of primates from the Eocene for which endocranial volumes can be estimated. Even fewer species are represented by high fidelity endocasts (i.e., complete, undistorted specimens with good surface preservation, often acquired through digital preparation), including the adapiforms *Notharctus tenebrosus*, *Smilodectes gracilis*, and *Adapis parisiensis* (Harrington *et al*., 2016), the omomyiforms *Microchoerus erinaceus* (Ramdarshan & Orliac, 2016) and *Rooneyia viejaensis* (Kirk *et al*., 2014). Descriptions of the endocasts of possible stem-primates from the Paleocene and Eocene, including the plesiadapiforms *Microsyops annectens* (Silcox *et al*., 2010) and *Ignacius graybullianus* (Silcox *et al*., 2009), form an important point of comparison to Eocene primate skulls. The combination of scarce data and robust interest in the underlying question means that each new digital endocast has the potential to substantially expand our understanding of primate brain evolution.

Necrolemur antiquus Filhol 1873 is a middle to late Eocene haplorhine primate first described from the Quercy Phosphorites in France and now recognized from multiple localities throughout western Europe (Godinot 2003; Minwer-Barakat *et al.*, 2015). Phylogenetically, *Necrolemur* is part of the family Omomyidae and is most closely related to the genera *Nannopithex* and *Microchoerus*, which together comprise the subfamily Microchoerinae. *Nannopithex* is thought to have given rise to *Necrolemur*, which is thought to have given rise to *Microchoerus* (Minwer-Barakat *et al*., 2015; 2017). *Necrolemur antiquus* is well-represented by dental remains and some isolated postcrania (Stehlin, 1916; Hürzeler, 1948; Simons & Russell, 1960; Simons, 1961; Godinot & Dagosto, 1983; Godinot, 2003). Like *Microchoerus*, it is often considered especially tarsier-like due to its elongated calcanei (Gebo, 1987; Boyer *et al*., 2013). While the endocast shape of *Necrolemur* has been known for more than 100 years (Stehlin, 1916; Hürzeler, 1948), estimates of endocranial volume (ECV) were not published until the latter half of the 20th century by Jerison (1973; 1979), Radinsky (1977), and Gurche (1982). Martin (1990) averaged the estimates made by these three authors and published an ECV of 3.8 cm^3 for *Necrolemur* (his Table 8.12). Martin's (1990) averaged ECV has been the preferred ECV in many subsequent studies of primate brain size (*e.g.* Silcox *et al*., 2009; Kirk *et al*., 2014; Ramdarshan & Orliac, 2016; Gilbert & Jungers, 2017).

Despite the frequent use of the 3.8 cm^3 ECV for *Necrolemur*, there are reasons to be cautious of this averaged value. Most evident among these is the nearly twofold difference between ECV estimates in the sample. Gurche (1982) estimated an ECV of only 2.65 cm^3 for *Necrolemur*, while Jerison (1973; 1979) and Radinsky (1977) made substantially larger estimates of 4.20 cm^3 and 4.35 cm^3 respectively. If these ECV differences were driven by true intraspecific variability, they would make the average more robust. However, tracing the history of how these ECV estimates were generated shows this is not the case (Figure 1). For Gurche (1982), the route from specimen to

estimated ECV is straightforward: water displacement of an endocast reconstructed from the Montauban 9 skull. According to Gurche (1978), this was accomplished by adding and carving plaster to a cast of the exposed portion of the Montauban 9 endocast, creating an artistic restoration that accounted for the thickness and dimensions of the surrounding cranial bones. The specimens underlying the ECV estimates of Jerison (1973; 1979) and Radinsky (1977) are more opaque. Both Jerison (1973; 1979) and Radinsky (1977) used double graphic integration – a method that relies on linear dimensions to model the brain as an elliptical cylinder – of an illustration in Radinsky (1970) to generate their ECV estimates. Radinsky's (1970) illustration is a composite of a figure published by Hürzeler (1948) and YPM specimen 18302 (a cast of BMNH M4490). In turn, Hürzeler's (1948) illustration was a reproduction of a figure published by Stehlin (1916), which was based on three *Necrolemur* specimens: Montauban 9, Montauban 10, and

Natural History Museum of Basel (NMB) QH 470. Thus, all three estimated ECVs for *Necrolemur* rely on the Montauban 9 specimen (Figure 1), so the three ECVs are not independent values representing within-species variation.

A more severe problem with averaging estimated ECVs for *Necrolemur* can be found in the composition details for Stehlin's (1916) figure. When describing the contribution of the three specimens, he writes that "Basel Q.H. 470 was decisive for the rendering of the facial skull and Montauban 9 for that of the brain skull. Montauban 10 was only used when the zygomatic arch and auditory canal and the I_1 were shown in the profile view (Stehlin, 1916: 1342; translated from German[1]). Finally, and most critically, in order to merge the Montauban specimens with Basel QH 470, "it was necessary to enlarge them somewhat more than the latter, based on the length of the row of molars" (Stehlin, 1916: 1341; translated from German[2]). Stehlin (1916) was focused on comparative brain shape and
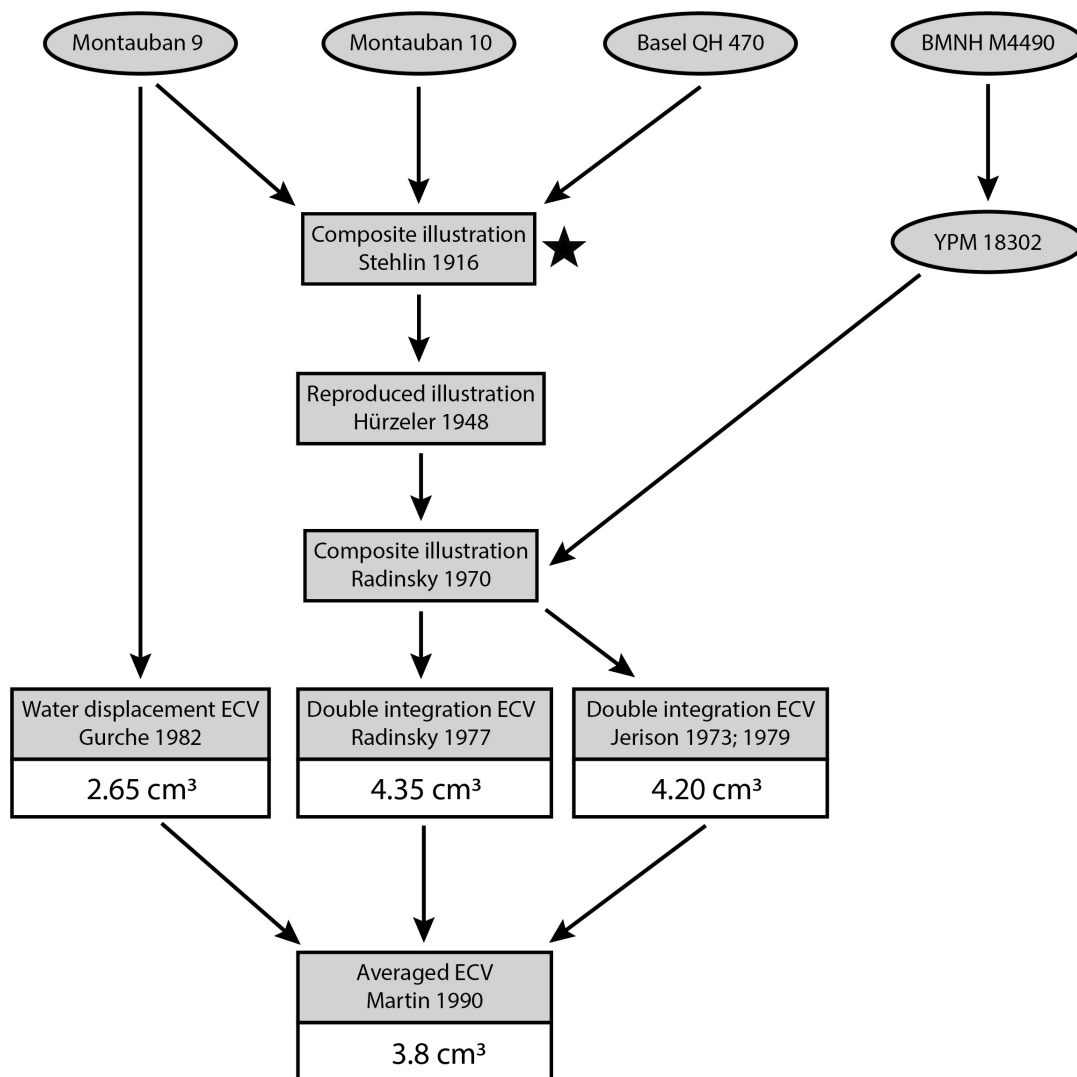
Figure 1. History of estimating endocranial volume in *Necrolemur antiquus*. Circles represent individual specimens, rectangles represent studies. In his composite drawing of the skull of *N. antiquus*, Stehlin (1916) (marked with a star) enlarged the neurocranium of the Montauban 9 skull to fit the splanchnocranium of Basel QH 470. Note that all estimated ECVs can be traced back to Montauban 9. In his composite drawing, Radinsky (1970) incorporated aspects of YPM 18302, a cast of BMNH M4490.

[1] "Für die Wiedergabe des Gesichtsschädels war Basel QH 470, für diejenige des Gehirnschädels Montauban 9 massgebend. Montauban 10 ist nur bei Darstellung des Jochbogens und des Gehörgangs, sowie des I1 in der Profilansicht beige zogen worden." (Stehlin, 1916, pg. 1342).
[2] "Um die Schädel Montauban 9 und 10 mit Basel QH 470 zu combinieren, war es nöthig sie etwas stärker zu vergrössern als den letztern, wobei als Basis die Länge der Backenzahnreihe gewählt wurde." (Stehlin, 1916, pg. 1341).

noted that increasing the size of Montauban 9 to match Basel QH 470 would not interfere with such comparisons. However, as far as we are aware, Stehlin's (1916) process for combining *Necrolemur* specimens has not been noted or accounted for by subsequent researchers who used his reconstruction to estimate endocranial volume. The implications are straightforward: the ECV estimates for *Necrolemur* made by Jerison (1973; 1979) and Radinsky (1977) are based on a composite illustration depicting an intentionally enlarged brain case. Because the most frequently used ECV estimate for *Necrolemur* in the last two decades has been Martin (1990)'s estimate (which averages the estimated ECVs of Jerison, 1973; 1979; Radinsky, 1977; and Gurche, 1982), it is quite likely the cited ECV value for *Necrolemur* has long been inflated.

Here, to provide an accurate and precise ECV estimate for *Necrolemur antiquus*, we describe the endocast of *Necrolemur antiquus* (MaPhQ 289, informally known as Montauban 9) after digital preparation. Endocast morphology is compared with those of other Eocene primates, particularly the omomyiforms *Microchoerus erinaceus* (Ramdarshan & Orliac, 2016) and *Rooneyia viejaensis* (Kirk *et al.*, 2014).

Institutional abbreviations

BMNH, Natural History Museum, London, UK; DU EA, Department of Evolutionary Anthropology Research Collection, Duke University, Durham, North Carolina, USA; Ma, Musée d'Histoire Naturelle Victor Brun, Montauban, France; MCZ, Museum of Comparative Zoology, Harvard University, Cambridge, Massachusetts, USA; NMB, Naturhistorisches Museum Basel, Basel, Switzerland; TMM, University of Texas Vertebrate Paleontology Collections, Austin, Texas, USA; UM, Université de Montpellier, Institut des Sciences de l'Evolution de Montpellier, Montpellier, France; USNM, United States National Museum (Smithsonian Institution), Washington D.C., USA; YPM, Yale Peabody Museum, New Haven, Connecticut, USA.

METHODS and MATERIALS

Specimens observed

The focal specimen of this study is MaPhQ 289 (informally known as Montauban No. 9), the skull of an adult *Necrolemur antiquus* originally described by Stehlin (1916). We also include comparisons to a number of other early primate endocasts (Table 1).

Observation methods and data accessibility

The current study was conducted entirely through digital observations. Musée d'Histoire Naturelle Victor Brun under authority of the city of Montauban, France (and with consent from R. Lebrun) granted access to a high-resolution X-ray computed tomography scan of MaPhQ 289. The specimen was scanned using a synchrotron X-ray source at European Synchrotron Radiation Facility (ESRF) facility by P. Tafforeau originally for research by R. Lebrun. The resulting 16-bit dataset is comprised of 1326 images with 876 by 646 pixels per image and the skull filling the majority of the image space. The voxels are cubic with a length of 30 μm. Gray values for bone and matrix spanned a range of approximately 25,000 - 61,000.

We provide a basic description of the scan below to confirm the specimen's state of preservation. The most important use of the scan was to create a digital endocast. Endocast reconstruction was accomplished by loading the tiff image series into the scientific data visualization program Avizo 8.1 (Visualization Sciences Group). In the "edit labelfield" module, the endocranial space was highlighted using the magic wand and brush tools in the XY plane. Occasionally, the "Interpolate" command was used to interpolate the shape of the endocranial space between hand-segmented slices. After interpolation, interpolated slices were examined visually for fit and re-drawn by hand if determined to be a poor match. Highlighted segments were then added to the label file and edited in the XZ and YZ planes if the bone/matrix boundary was found to be cleaner in another plane.

After smoothing the segments in the "Edit Labelfield" module, a three-dimensional mesh surface was generated from the label file using the "Generate Surface" module. The endocast was measured using the 2-D or 3-D ruler tool as appropriate. Volumes were measured using the "Surface Area Volume" tool. The circular fissure was used to distinguish the olfactory bulb from the cerebrum and olfactory bulb volume was measured after isolating the section using a 3-D lasso tool, reversing the selection, and deleting the remainder of the endocast. The raw tiff stack (doi.org/10.17602/M2/M114295) and the final endocast model (doi.org/10.17602/M2/M116186) are available on MorphoSource.org and the ESRF Heritage database.

RESULTS

### Specimen provenance and description

MaPhQ 289 is from the "Old Collections" of the Phosphorite deposits of Quercy, a set of specimens collected during mining operations in the late 1800s that lack specific locality information (Legendre *et al.*, 1997). Occurrences of *Necrolemur antiquus* at other European localities, such as La Bouffie in southern France, suggest a middle to late Eocene age for the species, specifically the European Paleogene mammalian biochron reference levels MP17 to MP20 (Godinot, 2003; Minwer-Barakat *et al.*, 2015). The skull is largely undistorted, but the neurocranium and splanchnocranium are separated by a break just inferior to the superior orbital margins (Figure 2). Portions of the frontal, left parietal, and left temporal bones are missing, exposing a natural endocast with the braincase. On the basicranium, the occipital is well preserved around the foramen magnum, but both auditory bullae have been broken open. The inferior portions of the sphenoid, including the pterygoid plates and the greater wings, are damaged or missing entirely. Both zygomatic arches are broken, but the superior and inferior margins of the right orbit are intact. Most of the left side of the face is missing, leaving only portions of the palate (including the alveolus for I^1 and a broken I^2) and the rostrum. The right maxilla preserves P^3-M^3, the root of I^2, and alveoli for P^2, C, and I^1. Despite some breakage, MaPhQ 289 is complete enough to provide a reasonable picture of the overall dimensions and shape of the skull.

Endocast description and comparisons

The exposed dorsolateral surfaces of the MaPhQ 289 endocast of *Necrolemur antiquus* was previously described by Gurche (1978). The virtual endocast (Figures 3, 4) now allows for a more complete description of the specimen. The endocast is only slightly longer along its anteroposterior axis than its mediolateral axis (even without considering the anteriorly positioned olfactory bulbs), giving it a fairly circular outline in

dorsal view. The endocast extends more than half the length of the skull (Figure 3). The olfactory bulbs are mostly complete and separated from the cerebrum by a well-developed circular fissure. The cerebral portion of endocast is lissencephalic (smooth without significant sulci and gyri apparent) and the Sylvian sulcus is the only clearly visible sulcus on the dorsal aspect (Figure 4B). The Sylvian sulcus is a fissure of the cerebrum separating the temporal lobe from the frontal and parietal lobes that is present in the brain of all extant primates (Elliot Smith, 1903) and the endocasts of all but one Eocene primate (*Smilodectes gracilis*) described to date (Gazin, 1965; Harrington *et al*., 2016). The cerebral portion is domed and extends superiorly above the olfactory bulbs and the orbits.

In this specimen, the cast of the orbitotemporal canal is not clearly visible on either of the temporal lobes (Figure 4E-F). The scan of the specimen reveals a possible indentation for the orbitotemporal canal on the ventrolateral surface of the endocranium, but the area was not clearly nor consistently delineated to segment a definitive cast of the canal on the endocast. In non anthropoid primates, the position of the orbitotemporal canal is closely associated with the position of the rhinal sulcus, which separates the paleocortical pyriform lobe from the neocortical portion of the temporal lobe (Gazin, 1965; Martin, 1990; Radinsky, 1970; Long *et al*., 2010). Unfortunately, the absence of a clear orbitotemporal canal in this specimen's endocast prevents the delineation of neocortical area. Posteriorly, the longitudinal fissure is hidden beneath a robust superior sagittal sinus. The midbrain is not exposed at the junction of the cerebrum and cerebellum, as it is covered by the occipital lobes, the confluence of sinuses, and the transverse sinuses (Figure 4B).
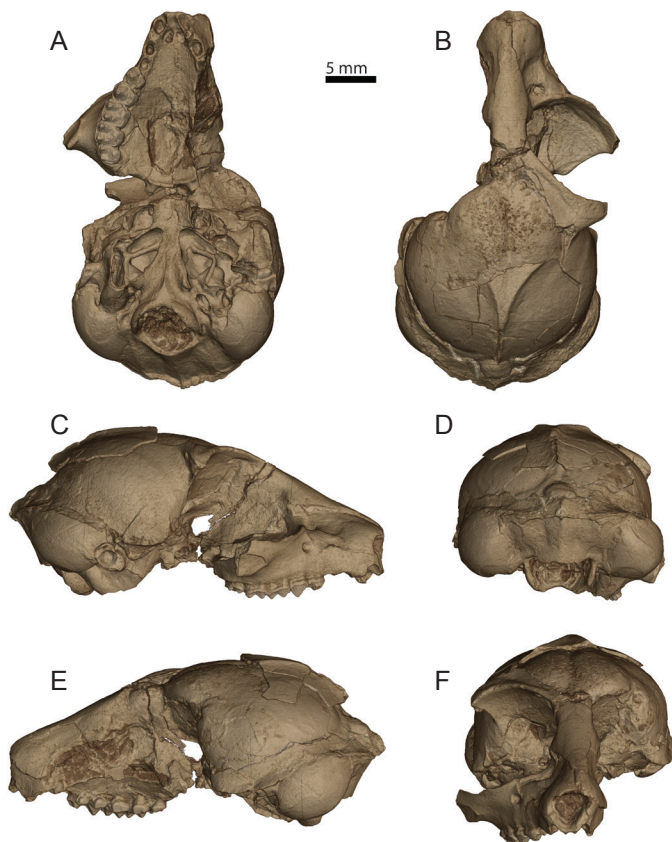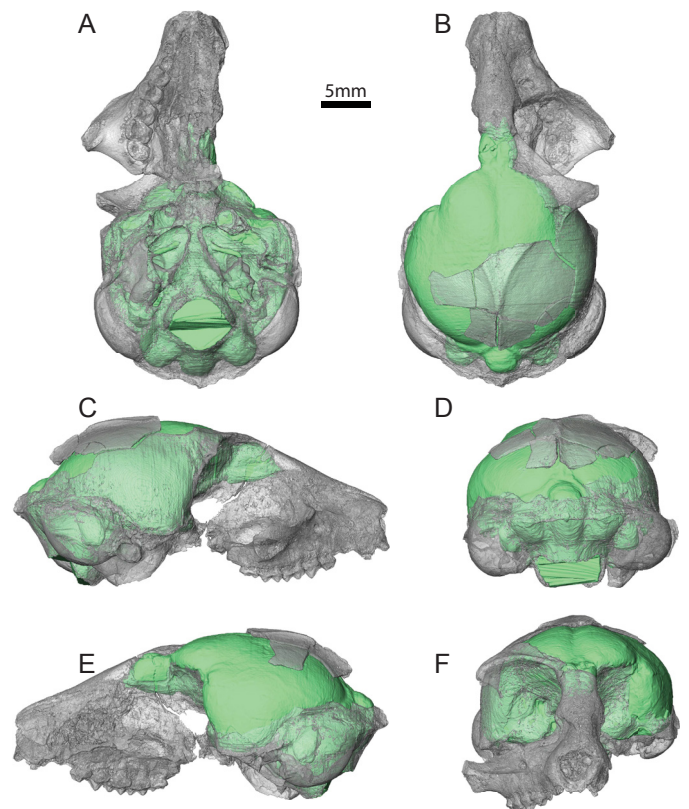
On the cerebellum, two pronounced paramedian fissures separate the medially placed vermis from two lateral lobes (Figure 4D). The fissura prima of the vermis is not distinguishable. The paraflocculi protrude ventrolaterally and are oval, with the dorsoventral axis larger than the anteroposterior axis. The paraflocculi are not visible in dorsal view.

On the ventral surface of the endocast (Figure 4A), casts of the jugular foramen (which would have contained cranial nerves IX-XI and the jugular vein) and the foramen ovale (which would have contained the mandibular branch of cranial nerve V) are clearly visible. Furthermore, casts of the internal acoustic meatus, which would have contained cranial nerves VII and VIII, are well preserved, as are the casts of the promontorial canal (containing the promontorial branch of the internal carotid artery), which was partially segmented independent of the endocast proper (Figure 4A, 4E-F). The inferior petrosal sinus is also visible, although ill-defined, and follows a path to the jugular foramen (Figure 4A, 4C). We were not able to discern clear boundaries of the optic foramen, sphenorbital fissure, or foramen rotundum from the CT images and they are thus not evident in the endocast. Gurche (1978) notes that some specimens of *Necrolemur* have a separated foramen rotundum and sphenorbital fissure, whereas they are merged in others. The condition found in this specimen is unclear to us from the scan. The cast of the hypophyseal (pituitary) fossa is too shallow and ill-defined for us to measure its dimensions (Figure 4A).

The overall shape and proportions of the *N. antiquus* endocast are very similar to that of *Microchoerus erinaceus*


Figure 2. Digital rendering of *Necrolemur antiquus* (MaPhQ 289) cranium imaged by SR-µCT at the ESRF. In **A**) ventral, **B**) dorsal, **C**) right lateral, **D**) posterior, **E**) left lateral, and **F**) anterior views. Scale bar is 5 mm.

Figure 3. Digital endocast of *Necrolemur antiquus* (MaPhQ 289) cranium imaged by SR-µCT at the ESRF. In **A**) ventral, **B**) dorsal, **C**) right lateral, **D**) posterior, **E**) left lateral, and **F**) anterior views. Scale bar is 5 mm.

(UM-PRR1771), from the late Eocene of Europe and often co-occurring with *Necrolemur* in collections of the Quercy deposits (Ramdarshan & Orliac, 2016). These endocasts share pronounced olfactory bulbs that extend anteriorly well beyond the frontal lobes, a noticeable Sylvian sulcus, lateral cerebellar lobes that project posteriorly beyond the occipital lobe of the cerebrum, and large and oval paraflocculi (Figure 5). The two endocasts differ notably in endocranial volume (4.26 cm^3 for *M. erinaceus* vs. 2.36 cm^3 for *N. antiquus*). The olfactory bulb volume of *N. antiquus* is approximately 2% of the endocast volume, slightly larger than the 1% previously reported for *M. erinaceus* (Table 1). Ramdarshan & Orliac (2016) argued that there are shallow lateral sulci parallel to the superior sagittal sinus present on the neocortex of *M. erinaceus*, but there are not similar depressions in *N. antiquus*. In *M. erinaceus*, the paraflocculi are visible in dorsal view, but these structures are not visible in *N. antiquus* (Figure 5). On the ventral surface, the structures present on *M. erinaceus* are broadly similar to those present on *N. antiquus*, but the former specimen preserves

better defined casts of the inferior petrosal sinus, hypophyseal fossa, and optic canal.

The endocasts of *N. antiquus* and *M. erinaceus* both differ from the late Eocene omomyiform *Rooneyia viejaensis* in their overall shape and dimensions. In *R. viejaensis*, the olfactory bulbs and cerebellum are hidden by overlying neocortical structures (the frontal lobes and occipital lobe respectively) in dorsal view, whereas these structures are clearly visible in dorsal view of the two microchoerine endocasts (Figure 5). *R. viejaensis* is more similar to *Microcebus murinus* in this respect. In dorsal view, the microchoerine endocasts have a circular profile, similar to *Tarsius* (Figure 5), as the maximum mediolateral breadth of their endocasts is slightly less than the maximum anteroposterior length of the cerebrum (Table 1). In contrast, the anteroposterior length of the cerebrum in *R. viejaensis* is greater than the mediolateral width (Table 1), giving its endocast a tear-drop shape in dorsal view (Figure 5), again similar to *M. murinus*.
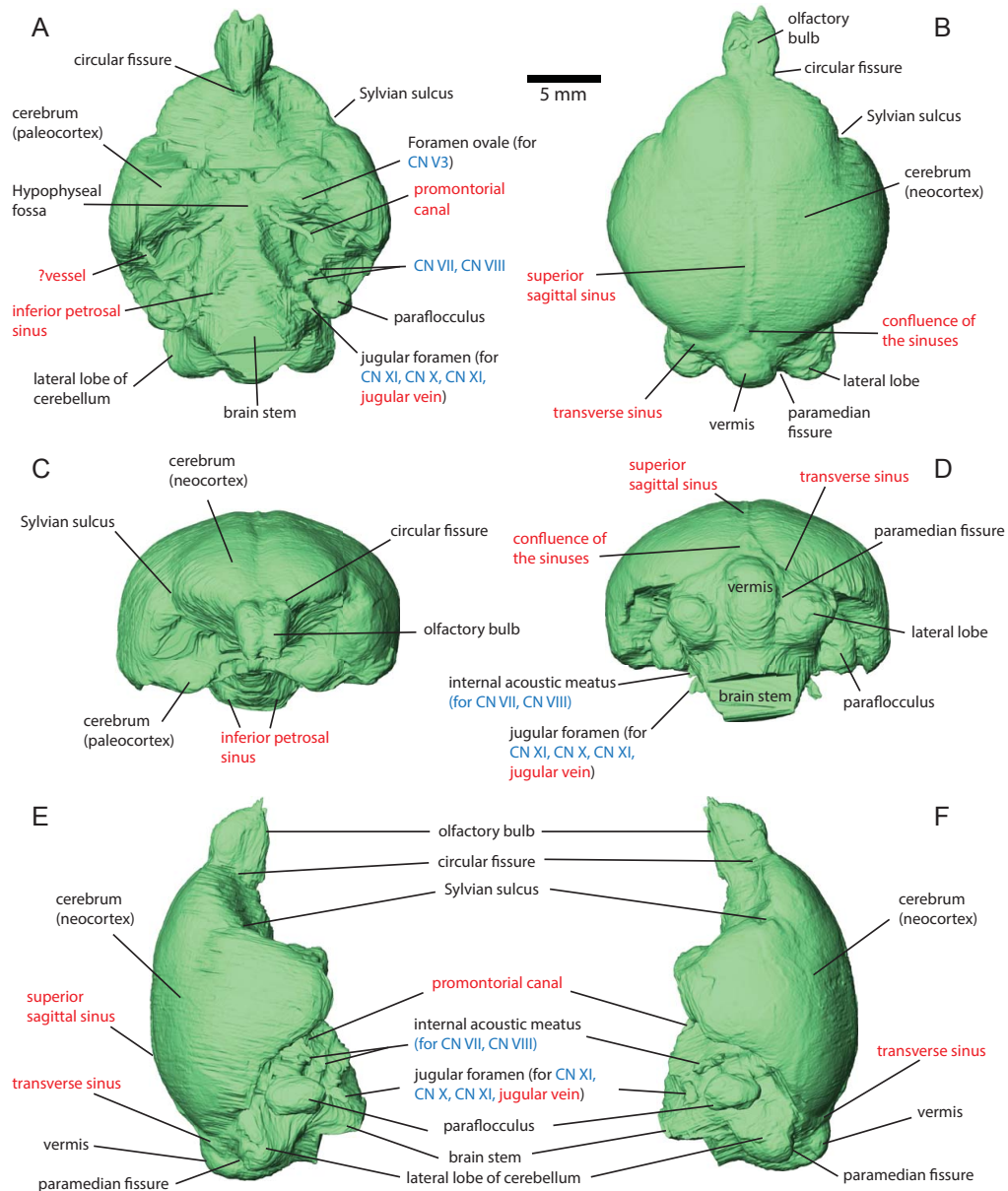
Figure 4. Features of the digital endocast of *Necrolemur antiquus* (MaPhQ 289). In **A**) ventral, **B**) dorsal, **C**) anterior, **D**) posterior, **E**) right lateral, and **F**) left lateral views. Scale bar is 5 mm.

Compared to the endocasts of extant primates of a similar size, the endocast of *N. antiquus* (and *M. erinaceus*) show less overlap of the olfactory bulbs or cerebellum by the cerebrum (Figure 5). The ECV of *N. antiquus* (2.36 cm³) is larger than that of *Microcebus murinus* (MCZ 44843; ECV = 1.7 cm³) and smaller than that of *Tarsius* sp. (DU EA 32; ECV = 3.6 cm³). The degree of lissencephaly of the endocast of *N. antiquus* is similar to that of *M. murinus* and *Tarsius*. In its degree of expansion, the temporal lobe appears more similar to that of *Tarsius* sp. (Figure 5). The endocast of *N. antiquus* exhibits some mediolateral expansion similar to *Tarsius*, but lacks the unique temporal lobe morphology seen in *Tarsius* (Figure 5).

Encephalization quotient

Encephalization quotients (EQs) are regression residuals that have been used historically to compare brain volumes among taxa with substantially different absolute body sizes. Specifically, they record the difference between an animal's observed brain volume and that expected as a function of its body mass (Jerison, 1973; Eisenberg, 1981). Though this method has limitations (*e.g.*, Gilbert & Jungers, 2017), encephalization quotients have been the most common method for characterizing relative brain size in primates and other mammals (*e.g.*, Jerison, 1973; Eisenberg, 1981). Existing literature (Radinsky, 1977; Jerison, 1979; Silcox *et al.*, 2009; 2010; Kirk *et al.*, 2014; Ramdarshan & Orliac, 2016; Gilbert & Jungers, 2017) indicates that *Necrolemur antiquus* has one of the largest EQs measured thus far among Paleocene and Eocene primates, surpassed only by *Rooneyia viejaensis*. For example, using the averaged endocranial volume of 3.8 cm³ and a body mass of 144 g (predicted using Martin's [1990] cranial length equation), Gilbert & Jungers (2017) calculated an EQ[3] of 1.75 for *N. antiquus*. This EQ is larger than those expressed by most other Eocene taxa (with the exception of *R. viejaensis*), is on the higher side of the EQ range seen in extant strepsirrhines, which range from 0.86 to 2.46 (Harrington *et al.*, 2016), and is comparable to those of tarsiers (e.g., *Tarsius spectrum* 1.74; *T. syrichta* 1.69) and other extant haplorhines, which range from 1.11 to 3.84 (Harrington *et al.*, 2016).

Adjusting the ECV for *Necrolemur antiquus* to 2.36 cm³ and keeping a predicted body mass of 144 g (generated with Martin's [1990] cranial length equation), the estimated EQ for *N. antiquus* drops from 1.75 to 1.08 (calculated with Eisenberg's [1981] primate-specific regression). Figure 6 shows the relationship between body mass (observed and predicted) and ECV in small-bodied (<500 g) euarchontans. Rather than being similar to tarsiers in its degree of encephalization, the updated ECV suggests *N. antiquus* was less encephalized than extant small-bodied strepsirrhines (e.g., *Cheirogaleus medius* 1.10), the tree shrews *Ptilocercus lowii* (1.88) and *Tupaia glis* (1.23), and other small-bodied Eocene taxa such as *Microchoerus erinaceus* (1.34) and *Rooneyia viejaensis* (1.64).

Encephalic blood supply

The new estimated ECV of *N. antiquus* also has interesting implications for encephalic blood supply. Boyer *et al.* (2016) showed a strong correlation between the size of the promontory canal and promontorial dominance of blood supply to the brain when controlling for endocast size. Among living primates with similar endocast sizes, the cross-sectional area of the promontorial canal predicts whether that canal would have contained a patent artery or just nerves in the adult. *Necrolemur* and *Microchoerus* both expressed relatively large promontorial canals for their endocast volumes and fit the pattern of living primates receiving blood from the promontorial artery.

Table 1. Endocast measurements for *Necrolemur antiquus* (MaPhQ 289) and other Eocene primates. Lengths are in millimeters (mm), areas in mm2, and volumes in mm3.

Taxon Specimen	*Necrolemur* MaPhQ 289	*Microchoerus* UM-PRR1771[a]	*Rooneyia* TMM 406887[b]	*Notharctus* MEAN[c]	*Smilodectes* MEAN[d]	*Adapis* NHM M1345[e]
Total endocast volume	2355	4260	7230	7623.3	8353.3	8810
Total endocast length	25.4	31.4	35	40.6	40.3	45.7
Maximum endocast width	19.4	23.1	25.6	26.8	28.6	36.6
Maximum endocast height	13.3	14.4	17.5	17	17.8	19
Maximum length of cerebrum	18.3	22.5	27.2	24.5	24.5	27
Maximum width of cerebellum	11.8	13.5	17.7	18.8	17.4	15.7
Olfactory bulb length	4.6	4.5	4.1	4.8	5.8	9.1
Olfactory bulb width	4.0	4.5	5.9	8.5	8.7	7.5
Length of endocast without olfactory bulbs*	21.6	26.8	30.1	35.8	33.9	36.6
Volume of olfactory bulbs	45.6	41	94	149	140.1	212
% of endocast composed of olfactory bulbs	1.94	0.96	1.3	1.95	1.68	2.41
Total surface area of endocast	1266	1866.7	2409.3	2963.3	3300	3170
Surface area of olfactory bulbs	63.7	81.2	102.6	159.3	208.7	195
Surface area of the neocortex	-	771.8	1054.6	905.3	1036.7	986
Neocortical ratio (without olfactory bulb surface area)	-	0.43	0.46	0.32	0.34	0.33
Telencephalic flexure (cranial base angle)	169°	161°	176°	171°	161°	187°

[a]Values from Ramdarshan & Orliac (2015)

[b]Measured from virtual endocast described by Kirk *et al.* (2015)

[c]Mean values for three adult specimens (AMNH 127167, USNM V 23277, USNM V 23278) described in Harrington *et al.* (2016)

[d]Mean values for three adult specimens (USNM V 17994, USNM V 17996, USNM V 21815) described in Harrington *et al.* (2016)

[e]Values from Harrington *et al.* (2016)

[3]Calculated with Eisenberg's (1981) primate-specific equation for encephalization quotient: $EQ = ECV/0.055*BM^{0.74}$.

The new, reduced endocast estimate does not change the conclusion about promontorial dominance in *Necrolemur*, but it does serve to substantially differentiate it from *Microchoerus*, to which it previously appeared similar. Before interpreting the significance of these differences, we thought it prudent to reassess promontorial canal size. The promontorial canals of three *Necrolemur* specimens show a narrow range of canal cross-sectional areas when measured at the proximodistal midpoint. MCZ BOM:8879 was measured by Boyer *et al.* (2016: Table S1) to have dimensions of 0.45 x 0.39 mm (scan available at https://doi.org/10.17602/M2/M13163). Based on the scan used for the endocast of this study, MaPhQ 289 measures 0.46 x 0.40 mm. Finally, YPM 011465 measures 0.43 x 0.33 mm (scan available at https://doi.org/10.17602/M2/M110555). We also remeasured UM-PRR1771 from the same scan used by Ramdarshan & Orliac (2016) to create their endocast. The proximodistal midpoint dimensions were 0.45 x 0.41 mm, slightly larger than those reported by Boyer *et al.*
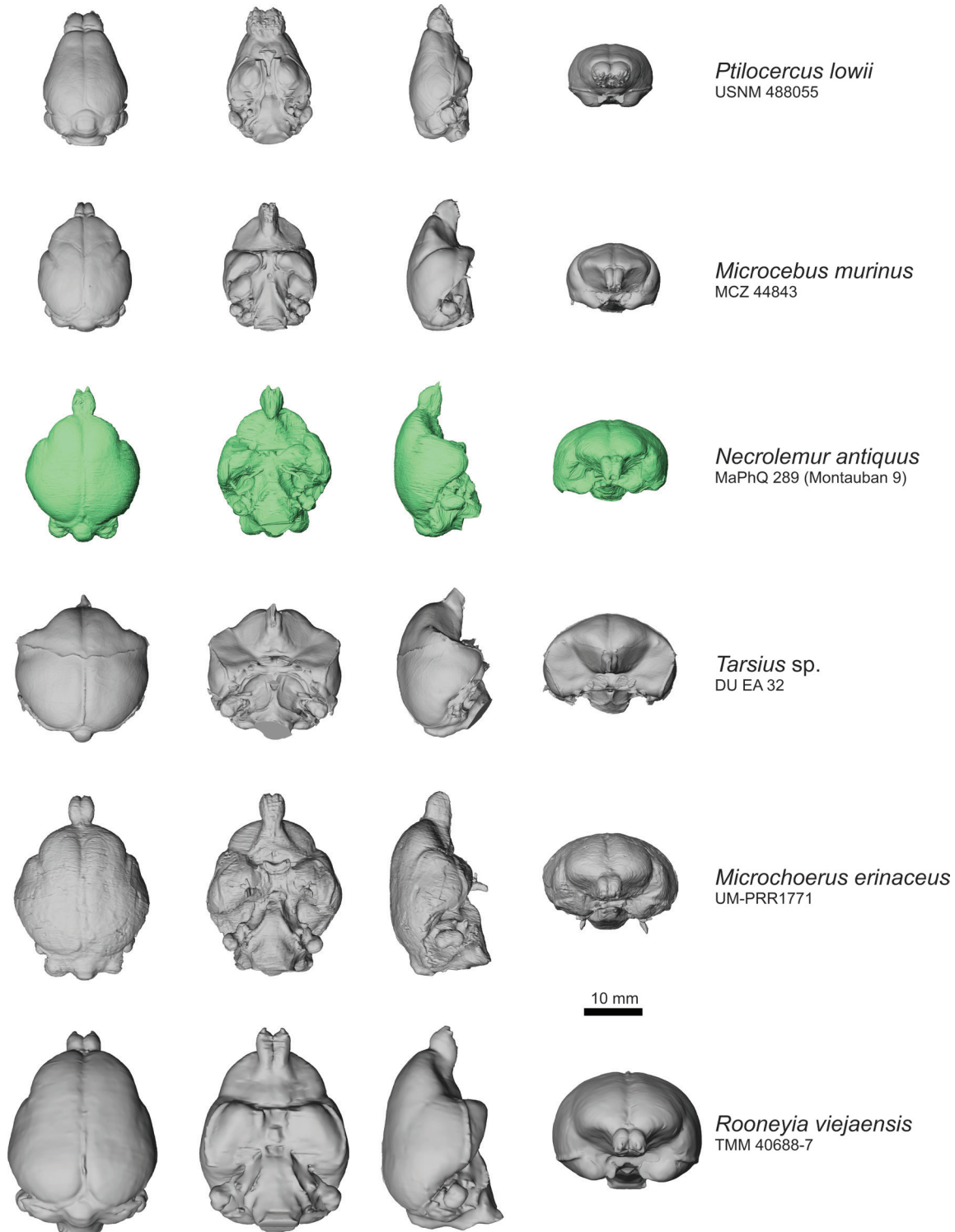
Figure 5. Comparison of euarchontan endocasts. From left to right, views are dorsal, ventral, right lateral, and anterior. To facilitate comparison of endocranial size and shape, the tubus olfactorius, a slender anterior extension of the olfactory fossa in *Tarsius*, is not included in the endocast. Scale bar is 10 mm.

(2016: Table S1) for the same specimen, using a different scan (scan available at https://doi.org/10.17602/M2/M13136), but nonetheless indicative that *Microchoerus* did not have a larger promontorial canal than *Necrolemur*, despite having a greater endocranial volume. Our new estimates suggest that as body size and brain size increased in *Microchoerus*, the relative contribution of the promontorial artery to encephalic blood requirements decreased. This may indicate a shift to greater reliance on vertebral arteries or other routes in the lineage leading to *Microchoerus*.

DISCUSSION AND CONCLUSION

While there are multiple crania known for *Necrolemur* (mentioned in Simons, 1961) and several descriptions of *Necrolemur*'s endocast morphology (Stehlin, 1916; Hürzeler, 1948; Radinsky, 1970; 1977; Jerison, 1979; Gurche, 1978; 1982), no endocasts have been digitally prepared for any species of the genus. Digital preparation of the MaPhQ 289 (Montauban 9) endocast reveals new morphology on the inferior surface of the endocast, but does not substantially alter previous morphological descriptions. However, in conjunction with careful reading of previous literature (Stehlin, 1916; Hürzeler, 1948), digital preparation reveals that the ECV for *Necrolemur* has likely been substantially overestimated for more than 40 years. Updating the ECV values for *Necrolemur*

shifts its EQ from being tarsier-like to more being cheirogaleid-like and makes it less encephalized than the similarly sized tree shrew *Tupaia* (assuming that cranial length serves as a reasonable proxy for body mass among Eocene primates).

The history of estimated endocranial volume in *Necrolemur* highlights the need for data standards for fossil endocasts. The complications of predicting body mass have long been recognized, as different prediction proxies and/or methods can yield substantially different EQs (*e.g.*, Gurche, 1982; Silcox *et al.*, 2009; Harrington *et al.*, 2016; Ramdarshan & Orliac, 2016; Gilbert & Jungers, 2017), but there has been less attention paid to the data quality of endocranial volumes. ECVs of fossil primates have generally been estimated with five different methods: digital preparation from CT data (Silcox *et al.*, 2009; Silcox *et al.*, 2010; Kirk *et al.*, 2014; Orliac *et al.*, 2014; Harrington *et al.*, 2016; Ramdarshan & Orliac, 2016; this study), infilling of the cranial cavity with mustard seed (*e.g.*, Gingerich & Martin, 1981), water displacement of a latex mold of the cranial cavity or restored models of endocasts (*e.g.*, Gurche, 1982), double graphic integration (*e.g.*, Jerison, 1977; Radinsky, 1979), or predicted from cranial dimensions such as length and width (*e.g.*, Martin, 1990). Of these alternatives, the first three methods likely have less attendant error than the last two, as they actually estimate an endocranial volume rather than predict one based on geometric relationships.

Based on the quality of the measurement techniques, published ECVs for *Tetonius homunculus* (obtained through
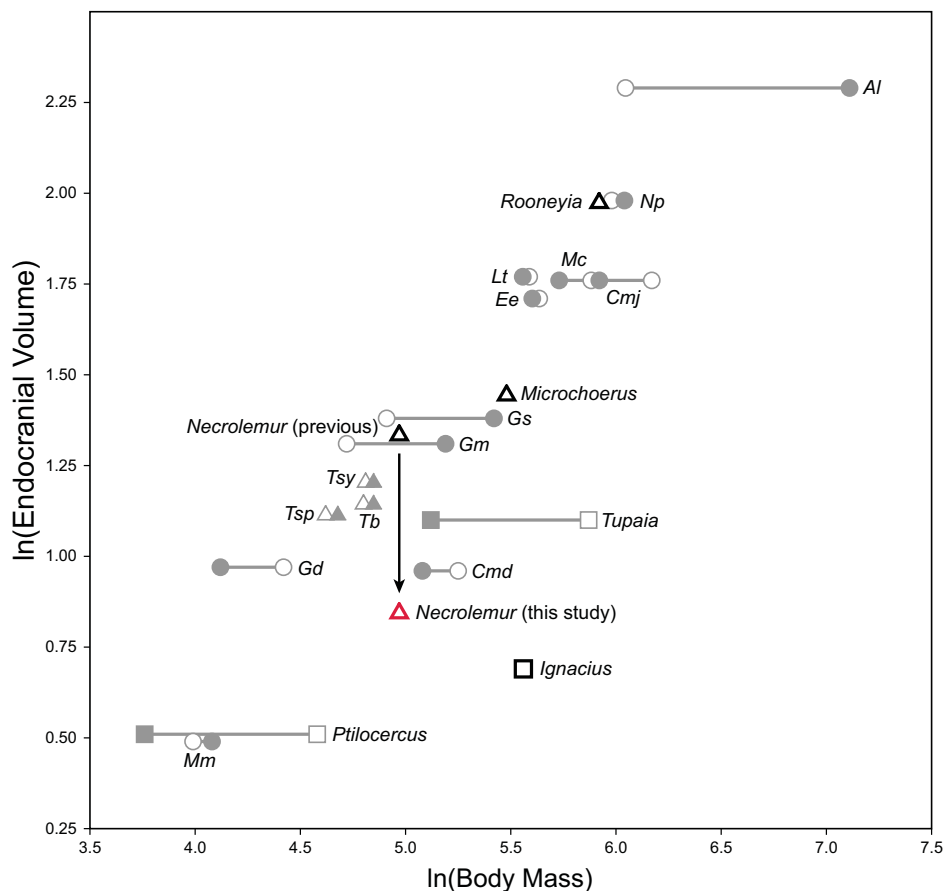
Figure 6. Endocranial volume and body mass (observed and predicted) in small-bodied (<500g) euarchontans. Filled symbols indicate observed species mean body mass, open symbols indicate species mean body mass predicted from cranial length using Martin's (1990) cranial length equation. Circles are strepsirrhines, triangles are tarsiiforms, squares are other euarchontans (dermopterans, scandentians, or plesiadapiforms). Al, *Avahi laniger*; Cmd, *Cheirogaleus medius*; Cmj, *Cheirogaleus major*; Ee, *Euoticus elegantulus*; Gd, *Galagoides demidoff*; Gm, *Galago moholi*; Gs, *Galago senegalensis*; Lt, *Loris tardigradus*; Mc, *Mirza coquereli*; Mm, *Microcebus murinus*; Np, *Nycticebus pygmaeus*; Tb, *Tarsius bancanus*; Tsp, *Tarsius spectrum*; Tsy, *Tarsius syrichta*.

double integration in Jerison [1979]) should be regarded with some skepticism, and published ECVs for *Leptadapis magnus* and *Pronycticebus gaudryi* (predicted from cranial dimensions in Martin [1990]) should be probably be excluded from broad comparative analyses. In the future, careful consideration of the quality of data required for estimating relative encephalization, both body masses and endocranial volumes, will enhance understanding of primate brain evolution.

BIBLIOGRAPHY

Barton, R.A., 2006. Primate brain evolution: integrating comparative, neurophysiological, and ethological data. Evolutionary Anthropology 15, 224-236. https://doi.org/10.1002/evan.20105

Clutton-Brock, T.H., Harvey, P.H., 1980. Primates, brains and ecology. Journal of Zoology 190, 309-323. https://doi.org/10.1111/j.1469-7998.1980.tb01430.x

Copes, L.E., Kimbel, W.H., 2016. Cranial vault thickness in primates: *Homo erectus* does not have uniquely thick vault bones. Journal of Human Evolution 90, 120-134. https://doi.org/10.1016/j.jhevol.2015.08.008

Dunbar, R.I., 1998. The social brain hypothesis. Evolutionary Anthropology 6, 178-190. https://doi.org/10.1002/(SICI)1520-6505(1998)6:5<178::AID-EVAN5>3.0.CO;2-8

Eliot Smith, G., 1903. On the morphology of the brain in Mammalia, with special reference to that of lemurs, recent and extinct. Transactions of the Linnean Society of London 2nd Ser.: Zoology 8, 319-432. https://doi.org/10.1111/j.1096-3642.1903.tb00497.x

Filhol, H., 1873. On fossil vertebrates found in the lime phosphate deposits of Quercy. Bulletin de la Société philomathique de Paris 10, 85-89.

Gazin, C.L., 1965. An endocranial cast of the Bridger Middle Eocene primate, *Smilodectes gracilis*. Smithsonian miscellaneous collections.149, 1-14.

Gilbert, C.C., Jungers, W.L., 2017. Comment on relative brain size in early primates and the use of encephalization quotients in primate evolution. Journal of Human Evolution 109, 79-87. https://doi.org/10.1016/j.jhevol.2017.04.007

Godinot, M., 2003. Variabilité morphologique et évolution des *Necrolemur* (Primates, Omomyiformes) des niveaux-repères MP 17 à MP 20 du sud de la France. Coloquios de Paleontologia. 1, 203-235.

Godinot, M., Dagosto, M., 1983. The astragalus of *Necrolemur* (Primates, Microchoerinae). Journal of Paleontology 57, 1321-1324.

Gurche, J.A., 1978. Early primate brain evolution. Master's thesis, University of Kansas.

Gurche, J.A., 1982. Early primate brain evolution. In: Armstrong, E., Falk, D. (Eds.), Primate Brain Evolution: Methods and Concepts. Springer, Boston, MA, pp. 227-246. https://doi.org/10.1007/978-1-4684-4148-2_15

Harrington, A.R., Silcox, M.T., Yapuncich, G.S., Boyer, D.M., Bloch, J.I., 2016. First virtual endocasts of adapiform primates. Journal of Human Evolution 99, 52-78. https://doi.org/10.1016/j.jhevol.2016.06.005

Healy, S.D., Rowe, C., 2007. A critique of comparative studies of brain size. Proceedings of the Royal Society B: Biological Sciences 274, 453-464. https://doi.org/10.1098/rspb.2006.3748

Hürzeler, J., 1948. Zur Stammesgeschichte der Necrolemuriden. Abhandlungen der Schweizerischen Paläontologischen Gesellschaft 66, 1-46.

Eisenberg, J.F., 1981. The Mammalian Radiations: An Analysis of the Trends in Evolution, Adaptation, and Behavior. University of Chicago Press, Chicago.

Jerison, H.J., 1973. Evolution of the Brain and Intelligence. Academic Press, New York. https://doi.org/10.1016/B978-0-12-385250-2.50018-3

Jerison, H.J., 1979. Brain, body and encephalization in early primates. Journal of Human Evolution 8, 615-635. https://doi.org/10.1016/0047-2484(79)90115-5

Kirk, E.C., Daghighi, P., Macrini, T.E., Bhullar, B.A.S., Rowe, T.B., 2014. Cranial anatomy of the Duchesnean primate *Rooneyia viejaensis*: New insights from high resolution computed tomography. Journal of Human Evolution 74, 82-95. https://doi.org/10.1016/j.jhevol.2014.03.007

Legendre, S., Sigé, B., Astruc, J.G., de Bonis, L., Crochet, J.Y., Denys, C., Godinot, M., Hartenberger, J.L., Lévêque, F., Marandat, B., Mourer-Chauviré, C., Rage, J.C., Remy, J.A., Sudre, J., Vianey-Liaud, M., 1997. Les phosphorites du Quercy: 30 ans de recherche. Bilan et perspectives. Geobios 30, 331-345. https://doi.org/10.1016/S0016-6995(97)80038-1

Long, A., Bloch, J.I., Silcox, M.T., 2015. Quantification of neocortical ratios in stem primates. American Journal of Physical Anthropology 157, 363-373. https://doi.org/10.1002/ajpa.22724

Martin, R.D., 1990. Primate Origins and Evolution: A Phylogenetic Reconstruction. Chapman and Hall, London. https://doi.org/10.1007/978-94-009-0813-0_3

Minwer-Barakat, R., Marigó, J., Moyà-Solà, S., 2015. *Necrolemur anadoni*, a new species of Microchoerinae (Omomyidae, Primates) from the Middle Eocene of Sant Jaume de Frontanyà (Pyrenees, Northeastern Spain). American Journal of Physical Anthropology 158, 730-744. https://doi.org/10.1002/ajpa.22867

Minwer-Barakat, R., Marigó, J., Femenias-Gual, J., Costeur, L., De

Esteban-Trivigno, S., Moyà-Solà, S., 2017. *Microchoerus hookeri* nov. sp., a new late Eocene European microchoerine (Omomyidae, Primates): new insights on the evolution of the genus *Microchoerus*. Journal of Human Evolution 102, 42-66. https://doi.org/10.1016/j.jhevol.2016.10.004

Radinsky, L., 1970. The fossil evidence of prosimian brain evolution. In: Noback, C. R., Montagna, W. (Eds.), The Primate Brain, Advances in Primatology, Vol. 1. Appleton Century Crofts, New York, pp. 781-798.

Radinsky, L., 1977. Early primate brains: facts and fiction. Journal of Human Evolution 6, 79-86. https://doi.org/10.1016/S0047-2484(77)80043-2

Ramdarshan, A. Orliac, M.J., 2016. Endocranial morphology of *Microchoerus erinaceus* (Euprimates, Tarsiiformes) and early evolution of the Euprimates brain. American Journal of Physical Anthropology 159, 5-16. https://doi.org/10.1002/ajpa.22868

Silcox, M.T., Dalmyn, C.K., Bloch, J.I., 2009. Virtual endocast of *Ignacius graybullianus* (Paromomyidae, Primates) and brain evolution in early primates. Proceedings of the National Academy of Sciences 106, 10987-10992. https://doi.org/10.1073/pnas.0812140106

Silcox, M.T., Benham, A.E., Bloch, J.I., 2010. Endocasts of *Microsyops* (Microsyopidae, Primates) and the evolution of the brain in primitive primates. Journal of Human Evolution 58, 505-521. https://doi.org/10.1016/j.jhevol.2010.03.008

Simons, E.L., 1961. Notes on Eocene tarsioids and a revision of some Necrolemurinae. Bulletin of the British Museum (Natural History) 5, 43-69.

Simons, E.L., Russell, D.E., 1960. Notes on the cranial anatomy of *Necrolemur*. Breviora 127, 1-14.

Simpson, G.G., 1944. Tempo and mode in evolution. Columbia University Press, New York.

Stehlin, H.G., 1916. Die Saugetiere des schweizeriscen Eocaens. Siebenter Teil, zweite Hälfte. Abhandlungen der Schweizerischen Paläontologischen Gesellschaft 41, 1299-1552.